DNA Mediated Energy Transfer from 4',6-Diamidino-2-phenylindole to Ru(II)[(1,10-phenanthroline)$_2$L]$^{2+}$: Effect of Ligand Structure

Mi Ryung Youn, Seok Joon Moon, Bae Wook Lee, Dong-Jin Lee,[†] Jong-Moon Kim, Seog K. Kim, and Chong-Soon Lee[‡,*]

Department of Chemistry, Yeungnam University, Kyoungsan City, Kyoung-buk 712-749, Korea
[†]Department of Advanced Materials and Environmental Engineering, Kyoungil University, Kyoungsan City, Kyoung-buk 712-701, Korea
[‡]Department of Biochemistry, Yeungnam University, Kyoungsan City, Kyoung-buk 712-749, Korea. [*]E-mail: cslee@yu.ac.kr
Received October 29, 2004

It was proposed that Ru(II)[(1,10-phenanthroline)$_2$dipyrido[3,2-a:2',3'-c]phenazine ([Ru(phen)$_2$DPPZ]$^{2+}$) complexes and 4',6-diamidino-2-phenylindole (DAPI) simultaneously bind to poly[d(A-T)$_2$] (*Biophysics. J.* **2003**, *85*, 3865). Förster type resonance energy transfer from excited DAPI to [Ru(phen)$_2$DPPZ]$^{2+}$ complexes was observed. In this study, we synthesized Δ- and Λ-[Ru(phenanthroline)$_2$dipyrido[3,2-a:2',3'-c]6-azaphenazine] ([Ru(phen)$_2$DPAPZ]$^{2+}$) at which the DNA intercalating ligand DPPZ was replaced and we studied its binding properties to poly[d(A-T)$_2$] in the presence and absence of DAPI using polarized spectroscopy and fluorescence techniques. All the spectroscopic properties of the [Ru(phen)$_2$DPAPZ]$^{2+}$-poly[d(A-T)$_2$] complex were the same in the presence and absence of DAPI that blocks the minor groove of polynucleotide, suggesting both Δ- and Λ-[Ru(phen)$_2$DPAPZ]$^{2+}$ complexes are located at the major groove of poly[d(A-T)$_2$]. On the other hand, in contrast with [Ru(phen)$_2$DPPZ]$^{2+}$, both Δ- and Λ-[Ru(phen)$_2$DPAPZ]$^{2+}$ exhibited almost twice the efficiency in the fluorescence quenching of DAPI that binds at the minor groove of poly[d(A-T)$_2$]. This observation indicates that the efficiency of the Förster type resonance energy transfer can be controlled by a small change in the chemical structure of the intercalated ligand.

Key Words : Ru complex, DNA, Energy transfer, 4',6-Diamidino-2-phenylindole, Binding mode

Introduction

Energy and charge transfer along the DNA stem has been a subject of intense study since the stacking of π-electrons of the DNA base was found to provide an effective medium for electron transfer.[1] Furthermore, energy transfer frequently occurs along the electron transfer reaction in biological systems. One of the early examples for the electron transfer along DNA appeared from the metallointercalators non-covalently bound to DNA. The luminescence intensity of a DNA intercalator Ru(II)[(1,10-phenanthroline)$_2$dipyrido-[3,2-a:2',3'-c]phenazine] (referred to as [Ru(phen)$_2$DPPZ]$^{2+}$, Figure 1) was efficiently quenched by an intercalated donor Rh(III)[(9,10-diimine phenanthrenequinone)$_2$phenanthrol-one], while the quenching was significantly less when DNA was modified by nonintercalating [Ru(NH$_3$)$_6$]$^{3+}$.[2-4] When an oligonucleotide was modified by ethidium derivatives and Rh(III)[(9,10-diimine phenanthrenequinone)$_2$bipyridine], electron transfer occurred at distance up to 30 Å.[5] Other types of charge transport also have been reported. For instance, hole injection into guanines of different oligo-nucleotide duplexes by a tethered Ru(II) complex, in which the tethered Ru(II) complex was adsorbed into the duplex grooves, was reported.[6] In contrast with electron transfer along the DNA stem between electron donor and acceptor,[4,5] a close contact between the Ru(II) complex and the guanine base was required for the hole transfer. Even in this condition, the hole injection was rather slow.

We recently demonstrated that excited energy of the minor groove binding drug 4',6-diamidino-2-phenylindole (referr-ed to as DAPI, Figure 1) transferred to various Ru(II) complexes via a Förster type resonance energy transfer when both drugs simultaneously bound to poly[d(A-T)$_2$].[7,8] The efficiency of the energy transfer was similar for both [Ru(phen)$_2$DPPZ]$^{2+}$ and [Ru(phen)$_2$benzodipyrido[3,2-a:2',3'-c]phenazine]$^{2+}$ complexes, whereas that of [Ru(phen)$_3$]$^{2+}$ was significantly lower. Considering the relationship be-tween the molecular structures of Ru(II) complexes and their binding modes to DNA, in which the long ligand of both [Ru(phen)$_2$DPPZ]$^{2+}$ and [Ru(phen)$_2$benzodipyrido[3,2-a:2',3'-c]phenazine]$^{2+}$ intercalate while [Ru(phen)$_3$]$^{2+}$ binds at the outside of DNA, it is conceivable that the intercalated ligand of Ru(II) complex is required for DNA base mediated Förster type resonance energy transfer. In that case, there might be possibilities to control the efficiency of the resonance energy transfer between DNA bound drugs and it will help the studies of electron or energy transfer reactions using DNA as mediation.

In this study, Δ- and Λ- isomer of the [Ru(phen)$_2$dipyrido-[3,2:2',3'-c]6-azaphenazine]$^{2+}$ (referred to as [Ru(phen)$_2$-DPAPZ]$^{2+}$: Figure 1), in which the extended dipyrido-phenazine of the [Ru(phen)$_2$DPPZ]$^{2+}$ was replaced by dipyrido-1-azaphenazine, was synthesized and the efficiency of the energy transfer from DAPI to this complex was investigated. It was found that the decrease in fluorescence intensity of the DAPI-poly[d(A-T)$_2$] complex upon binding

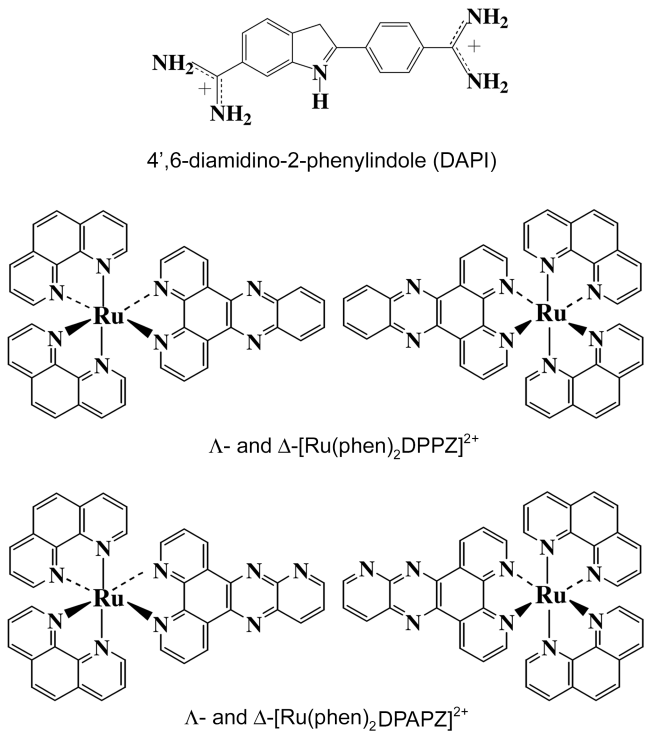

Figure 1. Molecular Structure of 4',6-diamidino-2-phenylindole, Λ- and Δ-$[Ru(phen)_2DPPZ]^{2+}$ and Λ- and Δ-$[Ru(phen)_2DPAPZ]^{2+}$.

of the Ru complexes can be elucidated by combining the sphere of action mechanism[9] and partial release of DAPI.

Experimental Section

Materials. Preparation of DAPI and poly[d(A-T)$_2$] was described elsewhere.[7,8] The $[Ru(phen)_2DPPZ]^{2+}$ was synthesized by a known procedure and the concentration was determined using an extinction coefficient of 20,000 M^{-1} cm^{-1} at 439 nm.[10] Δ- and Λ-$[Ru(phen)_2DPAPZ]^{2+}$ (DPAPZ = dipyrido[3,2-a:2',3'-c]6-azaphenazine) enantiomers (Figure 1) were prepared as described below. [Ru(phennanthroline)$_2$(1,10-phenanthroline-5,6-dione)]$^{2+}$ ($[Ru(phen)_2pq]^{2+}$) enantiomers were prepared as reported.[10] Then 0.10 g (0.1 mmol) of $[Ru(phen)_2pq]^{2+}$ and 0.2 mmol of 2,3-diaminopyridine were dissolved in 4 mL of acetonitrile/acetic acid mixture (5 : 5). The solution was refluxed at 80 °C for 2 hours, and the product was precipitated with ether after cooling. It was purified by a column chromatography of basic aluminia (Sigma).

Fluorescence Measurement. Fluorescence intensities were measured on a JASCO FP-777 spectrofluorometer. In the course of titration of the DAPI-poly[d(A-T)$_2$] complex by metal complexes, small aliquots of the latter were added to the sample solution and volume corrections were made. The emission intensities of DAPI were monitored through the excitation and emission at 360 nm and 450 nm, respectively. At this wavelength region, changes in DAPI fluorescence can be monitored without interference with the ruthenium fluorescence.

The fluorescence decay time of DAPI was measured using an IBH 500U Fluorescence Life Time System. The LED source of a nano-LED-03, which produces an excitation radiation at 370 nm with full width at a half-maximum of ~1.3 ns, was used to excite poly[d(A-T)$_2$] bound DAPI. The slit widths for both excitation and emission were 16 nm for fluorescence decay measurement.

Absorption, Linear and Circular Dichroism Spectrum. Measurement and data analysis of linear and circular dichroism (LD and CD) spectrum of the metal complexes that bound to DNA was described elsewhere.[7,8,11] CD spectra for the $[Ru(phen)_2DPAPZ]^{2+}$-DAPI-poly[d(A-T)$_2$] system were recorded on a JASCO-J715 spectropolarimeter displaying the CD in millidegree ellipticity. Absorption spectra were recorded on either a Hewlett-Packard 8452A diode array or a JASCO V-550 spectrophotometer. The path length was 10 mm for both absorption and CD measurements.

Results

Absorption, Linear and Circular Dichroism. DAPI shows the absorption band in the 280-410 nm region and its absorption maximum locates at 342 nm. The absorption spectrum of DAPI significantly overlaps with that of $[Ru(phen)_2DPAPZ]^{2+}$ complex hence we did not show the absorption spectra of DAPI and the mixture of DAPI and Ru(II) complex here.

Absorption spectrum of the Δ-$[Ru(phen)_2DPAPZ]^{2+}$ complex in the presence and absence of 30 μM and 150 μM poly[d(A-T)$_2$] in the MLCT band are compared in Figure 2. That obtained from Λ-enantiomer in the similar condition was the same as Δ-$[Ru(phen)_2DPAPZ]^{2+}$ complex (data not shown). At a glance, the shape of the absorption spectrum in the presence of different concentrations of poly[d(A-T)$_2$] is identical, indicating that the binding mode of the metal complexes is homogeneous in this concentration range.

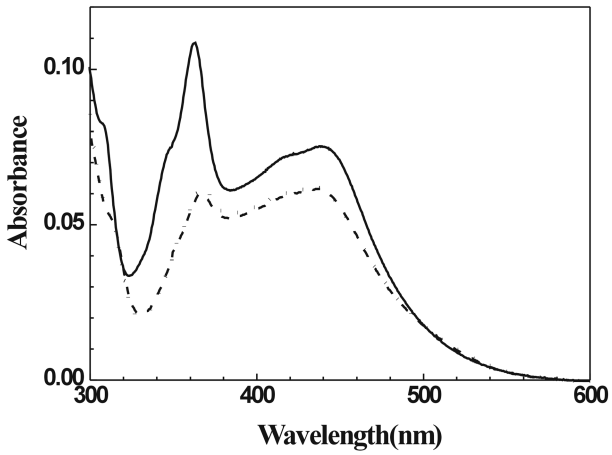

Figure 2. Absorption spectra of the Δ-$[Ru(phen)_2DPAPZ]^{2+}$ complex in the absence (solid curve) and presence of 30 μM (dashed curve) and 150 μM (dotted curve) of poly[d(A-T)$_2$]. [metal complex] = 3 μM.

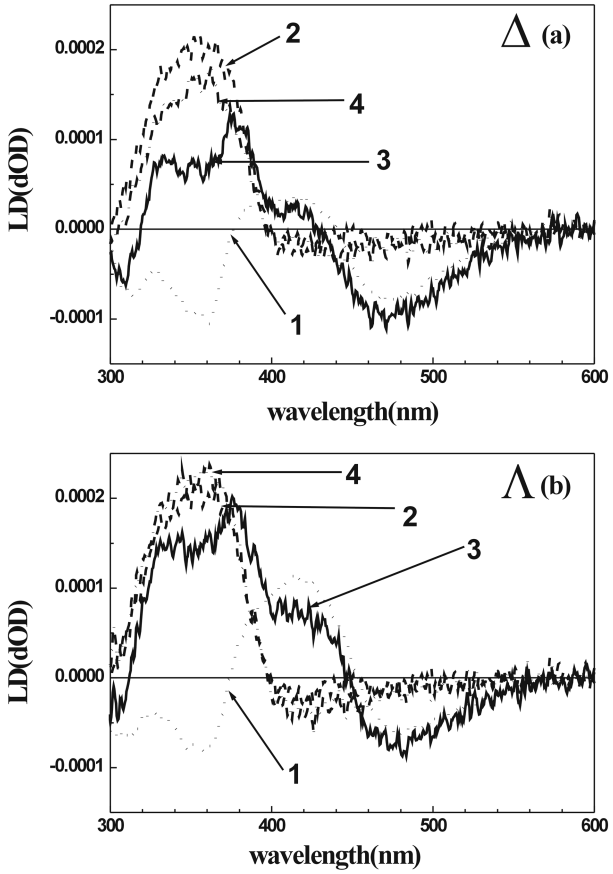

Figure 3. LD spectra of $[Ru(phen)_2DPAPZ]^{2+}$ (dotted curve; curve 1) and DAPI (dashed curve; curve 2) bound to poly[d(A-T)$_2$], sum of curve 1 and 2 (dotted and dashed curve; curve 4), and LD spectrum of $[Ru(phen)_2DPAPZ]^{2+}$-poly[d(A-T)$_2$]-DAPI complex (solid curve; curve 3). [DAPI] = 3 μM, [polynucleotide = 30 μM in nucleobases, [Ru(II) complex] = 3 μM.

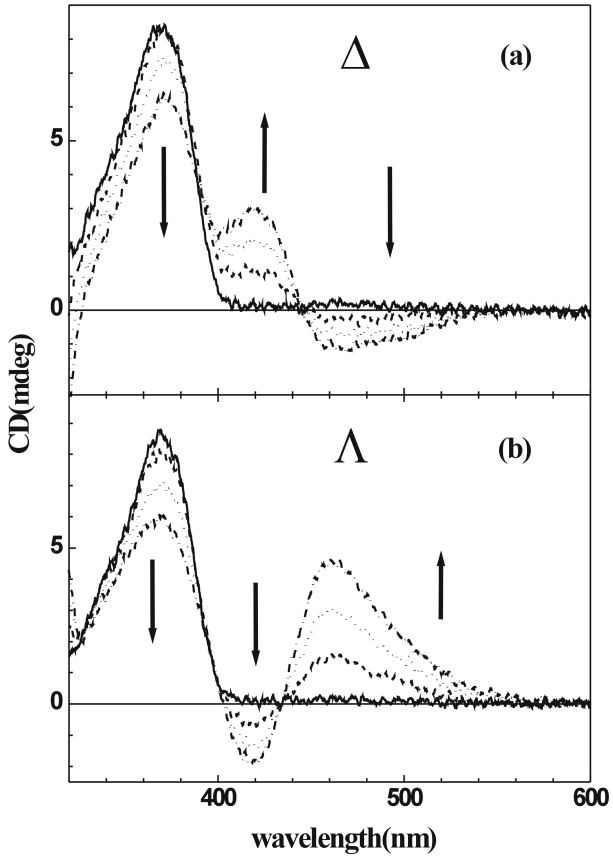

Figure 4. CD spectra of (a) Δ-$[Ru(phen)_2DPAPZ]^{2+}$ and (B) Λ-$[Ru(phen)_2DPAPZ]^{2+}$ complexes in the presence of DAPI-poly-[d(A-T)$_2$]. [DAPI] = 3 μM, poly[d(A-T)$_2$] = 30 μM in nucleobases. The concentrations of ruthenium complex increase to the arrow direction (0, 1, 2 and 3 μM).

$[Ru(phen)_2DPAPZ]^{2+}$complexes exhibit stronger absorption around 370 nm in the absence of poly[d(A-T)$_2$] compared to that of the $[Ru(phen)_2DPPZ]^{2+}$ complex, which is believed to be the transition of the extended ligand. The absorbance of both Δ- and Λ-enantiomers of the $[Ru(phen)_2DPAPZ]^{2+}$ complex in their entire MLCT region decreased upon binding to poly[d(A-T)$_2$], similarly with $[Ru(phen)_2DPPZ]^{2+}$ case. The hypochromism is particularly pronounced around 370 nm that corresponding to the absorption of extended ligand, suggesting the strong interaction of the extended ligand with the nucleobase. Overall shape of the LD spectrum is similar for Δ- and Λ-$[Ru(phen)_2DPAPZ]^{2+}$-poly[d(A-T)$_2$] complex and are also similar to those of the $[Ru(phen)_2DPPZ]^{2+}$-poly[d(A-T)$_2$] complexes.[12] A negative band in the DPAPZ absorption region followed by the positive and negative LD band in the MLCT band was apparent for both enantiomers (Figure 3). The magnitude of the positive band is somewhat larger for the Λ-isomer than Δ. A positive band in the 300-400 nm region was apparent when DAPI and the metal complexes co-exist (curve 4 in Figure 3), indicating that the presence of the metal complex did not result in a complete removal of DAPI.

The CD spectra of the $[Ru(phen)_2DPAPZ]^{2+}$-poly[d(A-T)$_2$] complexes in the presence and absence of DAPI as well as the DAPI-poly[d(A-T)$_2$] complex are depicted in Figure 4(a) and (b). DAPI has been well known to bind to the minor groove of DNA especially in the adenine-thymine rich region.[13-16] The concentration of DAPI in the complex was 3 μM and that of the polynucleotide was 30 μM being one DAPI molecule per five DNA base pairs. At this condition the minor groove is saturated by DAPI thereby providing complete blocking of the minor groove. In the previous studies, it was reported that DAPI and enantiomeric $[Ru(phen)_2DPPZ]^{2+}$ complexes simultaneously bind to poly[d(A-T)$_2$] at, respectively, the minor and major groove, and induces a Förster type energy transfer.[7,8] As it is shown in Figure 4, the presence of DAPI did not affect the CD spectrum of both enantiomers of the $[Ru(phen)_2DPAPZ]^{2+}$ complex at a low metal complex concentration. However, an increase in the concentration of the $[Ru(phen)_2DPAPZ]^{2+}$ complex results in the partial release of DAPI which is in contrast with $[Ru(phen)_2DPPZ]^{2+}$ case: the presence of 3 μM of the $[Ru(phen)_2DPPZ]^{2+}$ complex did not affect the shape of the DAPI CD.

Fluorescence and Fluorescence Decay Time Measurements. If the quenching of DAPI fluorescence follows a simple static or dynamic mechanism, a straight line should

appear when the ratio of the fluorescence intensity in the absence of quencher (F_0) to that in the presence (F) is plotted with respect to the quencher concentration ([Q]), which is called the Stern-Volmer plot:

$$F_0/F = 1 + K_{SV}[Q]$$

where K_{SV} is either the dynamic or static quenching constant. However, an upward bending curve is often observed in the Stern-Volmer plot, which can be understood as a combination of static and dynamic quenching. In this case, the quenching efficiency can be explained by:

$$\frac{F_0}{F} = (1 + K_S[Q])(1 + K_D[Q])$$

where K_S and K_D represent static and dynamic quenching constants, respectively. Solving the above equation results in:

$$\frac{(F_0/F - 1)}{[Q]} = (K_S + K_D)\, K_S K_D[Q]$$

Therefore, K_S and K_D can be obtained from the slope and intercept of the plot $(F_0/F - 1)/[Q]$ *vs* $[Q]$.

The fluorescence intensity of DAPI-poly[d(A-T)$_2$] complex gradually decreased as the concentrations of the [Ru(phen)$_2$DPAPZ]$^{2+}$ complexes increase. A decrease in fluorescence intensity with respect to the concentration of the metal complexes is shown in Figure 5(a) as the Stern-Volmer type plot where the metal complexes are Δ- and Λ-[Ru(phen)$_2$DPAPZ]$^{2+}$ and, for comparison, [Ru(phen)$_2$DPPZ]$^{2+}$. All metal complexes exhibit upward bending curves in the Stern-Volmer plot, indicating that the quenching of DAPI fluorescence by the metal complexes can not be explained by a simple dynamic or static mechanism. It was noticed that the quenching efficiency is higher for the [Ru(phen)$_2$-DPAPZ]$^{2+}$ complex compared to that of the [Ru(phen)$_2$-DPPZ]$^{2+}$. As it was observed for [Ru(phen)$_2$DPPZ]$^{2+}$, the Λ-[Ru(phen)$_2$DPAPZ]$^{2+}$ always exhibited a higher quenching efficiency than Δ-[Ru(phen)$_2$DPAPZ]$^{2+}$. Although the upward bending curve in the Stern-Volmer plot is usually explained by a combination of the static and dynamic quenching mechanism that is represented as a straight line in the (F_0/F-1)/[Q] *vs* [Q] plot, an upward bending curve was observed even in this plot (Figure 5(b)), suggesting that the extent of decrease in fluorescence intensity is far larger and an additional quenching mechanism is involved. There is a

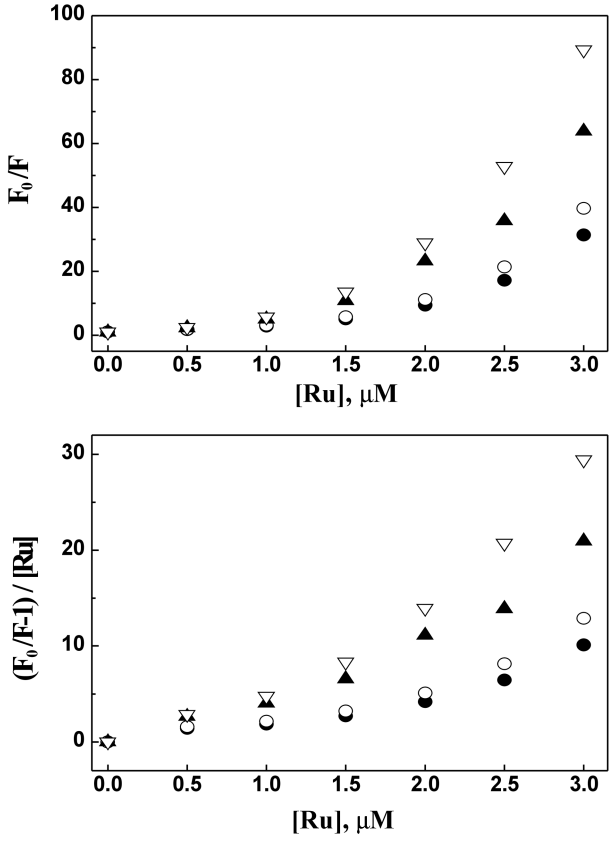

Figure 5. Fluorescence intensity of DAPI bound to poly[d(A-T)$_2$] as a function of concentration of ruthenium complex: (closed circles) Δ-DPPZ; (open circles) Λ-DPPZ; (closed triangles) Δ-DPAPZ; (open triangles) Λ-DPAPZ. Excitation and emission wavelengths were 345 and 460 nm, respectively. Slit widths were 3 nm for excitation and emission. [DAPI] = 3 μM, poly[d(A-T)$_2$] = 30 μM in nucleobase.

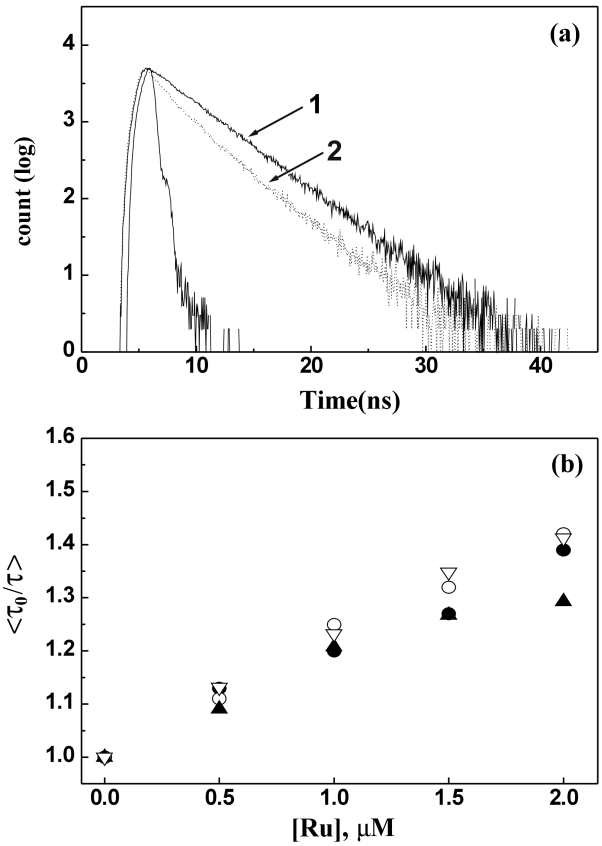

Figure 6. (a) Fluorescence decay profile of DPAI-poly[d(A-T)$_2$] in the absence (curve 1) and presence of [Ru(phen)$_2$DPAPZ]$^{2+}$ (curve 2). Excitation at 370 nm by LED source and emission at 460 nm. Slit widths were 16 nm for excitation and emission. [DAPI] = 3 μM, [Ruthenium] = 3 μM. and poly[d(A-T)$_2$] = 30 μM in nucleobase. (b) The ratio of average decay time of DAPI-poly[d(A-T)$_2$] in the absence of ruthenium complex to their presence. Symbol assignment is the same as in Fig. 5.

Table 1. Luminescence decay time of DAPI bound to poly[d(A-T)$_2$] in the presence of Δ- and Λ-[Ru(phen)$_2$DPPZ]$^{2+}$ and [Ru(phen)$_2$DPAPZ]$^{2+}$

	DPPZ								DPAPZ							
	Δ				Λ				Δ				Λ			
R[a]	t[b]1	a[c]1	t2	a2	t1	a1	t2	a2	t1	a1	t2	a2	t1	a1	t2	a2
0.0	1.12	2.41	3.89	97.59	1.23	3.55	3.89	96.45	1.11	2.06	3.87	97.94	1.07	2.01	3.86	97.99
0.5	1.04	7.04	3.69	92.96	1.11	17.03	3.72	82.97	1.33	12.77	3.70	87.23	0.88	7.68	3.65	92.32
1.0	1.03	15.43	3.47	84.57	1.14	24.00	3.48	76.00	0.97	20.02	3.64	79.98	1.06	14.56	3.54	85.44
1.5	0.97	26.84	3.46	73.16	0.83	28.71	3.24	71.29	1.01	24.82	3.39	75.18	1.03	18.13	3.40	81.87
2.0	0.83	35.34	3.44	64.66	0.80	42.45	3.23	57.55	1.06	37.33	3.42	62.67	0.92	24.29	3.34	75.71

[a]R = [Metal complex]/[DNA base]; [DNA base] = 30 μM, [DAPI] = 3 μM. [b]decay time in nanosecond. [c]amplitude in percentage

possibility that the small portion of released DAPI from DNA due to [Ru(phen)$_2$DPAPZ]$^{2+}$ binding may influence the quenching mechanism. Here we did not consider the effect of unbound DAPI to the quenching mechanism because there is no method established to consider the contribution of unbound DAPI. It is noteworthy that none of the metal complexes showed quenching activity for the DAPI in the absence of poly[d(A-T)$_2$] (data not shown), suggesting that the simultaneous binding of DAPI and the metal complexes are required for the transfer of excited energy of DAPI to the metal complexes. It was also noticed that, in contrast with the [Ru(phen)$_2$DPPZ]$^{2+}$ complex case, the Λ-[Ru(phen)$_2$DPAPZ]$^{2+}$ produced no fluorescence, neither in the presence nor in the absence of DAPI and/or poly[d(A-T)$_2$].

The representative fluorescence decay profiles of the DAPI-poly[d(A-T)$_2$] complex in the presence and absence of metal complexes are depicted in Figure 6(A). The fluorescence decay profiles of DAPI and DAPI-poly[d(A-T)$_2$] complexes were well studied.[17,18] In a buffer solution at pH 7, the decay of DAPI was decomposed using two exponentials having short and long lifetime values of approximately 0.2 ns and 2.8 ns, respectively. In the presence of poly[d(A-T)$_2$], the long lifetime component is dominant while a short lifetime component is dominant in the absence of poly[d(A-T)$_2$]. Furthermore, a gradual increase of a long lifetime component was observed with increasing poly[d(A-T)$_2$] concentration, indicating that DNA binding stabilizes the long lifetime component due to the enhanced shielding of DAPI from solvent water molecules.

The fluorescence decay times of DAPI complexed with poly[d(A-T)$_2$] were in the presence of [Ru(phen)$_2$DPPZ]$^{2+}$ and [Ru(phen)$_2$DPAPZ]$^{2+}$ are listed in Table 1. In the absence of Ru(II) complex, poly[d(A-T)$_2$] bound DAPI showed two lifetimes; shorter one is about 1 ns and longer one about 4 ns, respectively. The addition of the [Ru(phen)$_2$-DPAPZ]$^{2+}$ complexes shortened both short and long decay time: from 3.86 ns to 3.46 ns for long component and 1.19 ns to 0.89 ns for short components. The decay time changes upon the concentration of the Ru(II) complexes are depicted in Figure 5(b), where the average decay time is defined by, for two components decay, $\bar{\tau} = (a_1\tau_1^2 + a_2\tau_2^2)/(a_1\tau_1 + a_2\tau_2)$.[9] In contrast with the fluorescence quenching profile, [Ru(phen)$_2$DPAPZ]$^{2+}$ enantiomers showed a similar effect in shortening the average decay time with the [Ru(phen)$_2$-DPPZ]$^{2+}$ complex.

Discussion

Upon binding to poly[d(A-T)$_2$], both Δ- and Λ-[Ru(phen)$_2$DPAPZ]$^{2+}$ exhibited hypochromism in the entire drug absorption region, which is particularly pronounced in the DPAPZ absorption region. Corresponding LD signal in the DPAPZ absorption region is negative. Both LD and CD characteristics are essentially the same in the presence and absence of DAPI, indicating that DAPI and the metal complexes are simultaneously bound to poly[d(A-T)$_2$]. These observations and other spectral properties including CD are similar to those of the [Ru(phen)$_2$DPPZ]$^{2+}$ complexes. Therefore, it may be concluded that the binding mode of the [Ru(phen)$_2$DPAPZ]$^{2+}$ complex is similar to that of [Ru(phen)$_2$DPPZ]$^{2+}$, where the two phenanthroline ligands locate in the major groove with its extended ligand intercalated. However, it should be noted that as it was seen in the CD titration, the binding of the [Ru(phen)$_2$DPAPZ]$^{2+}$ complex results in the partial release of DAPI in contrast with [Ru(phen)$_2$DPPZ]$^{2+}$ complexes: the binding of 3 μM metal complex to 30 μM poly[d(A-T)$_2$], which corresponds to one metal complex per five nucleobase pairs, resulting in a 20% release of the DAPI for both complexes as it is judged by the CD intensity at 360 nm.

In contrast with spectral properties, significant differences in the efficiency of fluorescence quenching experiments were noticed. [Ru(phen)$_2$DPAPZ]$^{2+}$ showed about two times greater quenching efficiency than [Ru(phen)$_2$DPPZ]$^{2+}$, while the effect in the change in the fluorescence decay time is similar for all complexes. The quenching of the fluorescence intensity of the poly[d(A-T)$_2$] bound DAPI by various metal complexes was elucidated by a Förster type resonance energy transfer.[8] It occurs when the energy of the fluorescence emission of the fluorophore coincides with the absorption energy of the near-by quencher molecule. In the [Ru(phen)$_2$DPPZ]$^{2+}$ case, the distance between DAPI and [Ru(phen)$_2$DPPZ]$^{2+}$ was calculated as 0.64*R*, where *R* denotes the Förster distance.[19] Since the quenching of the DAPI fluorescence cannot be explained by the combination

of static and dynamic mechanisms, *i.e.*, Förster type resonance energy transfer alone, there must be another path for DAPI to lose its excited energy or quantum yield. Although the distance and relative orientation of the acceptor molecule relative to the donor molecule is the most important factor, we did not find any difference in binding mode between the $[Ru(phen)_2DPPZ]^{2+}$ and $[Ru(phen)_2DPAPZ]^{2+}$ molecules, indicating that distance and orientation are not the factors explaining the difference in quenching efficiency. However, the binding of the $[Ru(phen)_2DPAPZ]^{2+}$ complex evidently induces the partial release of DAPI. Partial release of DAPI from poly[d(A-T)$_2$] is more efficient for the $[Ru(phen)_2DPAPZ]^{2+}$ than $[Ru(phen)_2DPPZ]^{2+}$. Since the quantum yield of the polynucleotide-free DAPI is far lower than that of the poly[d(A-T)$_2$] bound ones, partial release of DAPI can be a possible reason for extra loss of the fluorescence intensity of the DAPI-poly[d(A-T)$_2$] complex.

Acknowledgement. This work was supported by Korea Research Foundation (Grant no. KRF 2002-070-C00053).

References

1. Boon, E.; Barton, J. K. *Curr. Opin. Struct. Biol.* **2000**, *12*, 320.
2. Murphy, C. J.; Arkin, M. R.; Jenkins, Y.; Ghatlia, N. D.; Bossmann, S. H.; Turro, N. J.; Barton, J. K. *Science* **1993**, *262*, 1025.
3. Murphy, C. J.; Arkin, M. R.; Ghatlia, N. D.; Bossmann, S.; Turro, N. J.; Barton, J. K. *Proc. Natl. Acad. Sci. USA* **1994**, *91*, 5315.
4. Meade, T.; Kayyem, J. *Angew. Chem. Int. Ed. Engl.* **1995**, *34*, 352.
5. Kelley, S. O.; Holmlin, R. E.; Stemp, E. D. A.; Barton, J. K. *J. Am. Chem. Soc.* **1997**, *119*, 9861.
6. Garcia-Fresnadillo, D.; Boutonnet, N.; Schumm, S.; Moucheron, C.; Kirsch-De Mesmaeker, A.; Defrancq, E.; Constant, J. F.; Lhomme, J. *Biophys. J.* **2002**, *82*, 978.
7. Yun, B. H.; Kim, J.-O.; Lee, B. W.; Lincoln, P.; Nordén, B.; Kim, J.-M.; Kim, S. K. *J. Phys. Chem. B* **2003**, *107*, 9858.
8. Lee, B. W.; Moon, S. J.; Youn, M. R.; Kim, J. H.; Jang, H. G.; Kim, S. K. *Biophys. J.* **2003**, *85*, 3865.
9. Lakowicz, J. R. *Principles of Fluorescence Spectroscopy*; Plenum Press: New York, 1999; p 130.
10. Hiort, C.; Lincoln, P.; Nordén, B. *J. Am. Chem. Soc.* **1993**, *115*, 3448.
11. Hwangbo, H. J.; Lee, Y.-A.; Park, J. H.; Lee, Y. R.; Kim, J.-M.; Yi, S. Y.; Kim, S. K. *Bull. Korean Chem. Soc.* **2003**, *24*, 579.
12. Cho, C.-B.; Cho, T.-S.; Kim, S. K.; Kim, B.-J.; Han, S. W.; Jung, M.-J. *Bull. Kor. Chem. Soc.* **2000**, *21*, 995.
13. Hard, T.; Fan, P.; Kearns, D. R. *Photochem. Photobiol.* **1990**, *51*, 77.
14. Eriksson, S.; Kim, S. K.; Kubista, M.; Nordén, B. *Biochemistry* **1993**, *32*, 2987.
15. Larsen, T. A.; Goodsell, D. S.; Cascio, D.; Grzeskowiak, K.; Dickerson, R. E. *J. Biomol. Struct. Dyn.* **1989**, *7*, 477.
16. Parolin, C.; Zanotti, G.; Palu, G. *Biochem. Biophys. Res. Commun.* **1995**, *208*, 332.
17. Barcellona, M. L.; Cardiel, G.; Gratton, E. *Ital. J. Biochem.* **1990**, *39*, 179A.
18. Barcellona, M. L.; Cardiel, G.; Gratton, E. *Biochem. Biophys. Res. Commun.* **1990**, *170*, 270.
19. Lakowicz, J. R. *Principles of Fluorescence Spectroscopy*; Plenum Press: New York, 2001; p 367.